https://doi.org/10.5194/bg-2020-145
Preprint. Discussion started: 20 May 2020

Biogeosciences Discussions
Open Access
EGU

New insights into mechanisms of sunlight-mediated high-temperature accelerated diurnal production-degradation of fluorescent DOM in lake waters

by

Yijun Liu[1,2], Jie Yuan[3], Fu-Jun Yue[1,2], Si-Liang Li[1,2], Baoli Wang[1,2], Mohammad Mohinuzzaman[1,2], Xuemei Yang[1,2], Nicola Senesi[4], Xinyu Lao[1,2], Longlong Li[1,2], Cong-Qiang Liu[1,2], Rob M. Ellam[5,1], and Khan M.G. Mostofa[*1,2],

[1]Institute of Surface-Earth System Science, Tianjin University, 92 Weijin Road, Tianjin 300072, China.

[2]Tianjin Key Laboratory of Earth Critical Zone Science and Sustainable Development in Bohai Rim, Tianjin University, 92 Weijin Road, Tianjin 300072, China.

[3]Key Laboratory of Earth and Planetary Physics, Institute of Geology and Geophysics, Chinese Academy of Sciences, Beitucheng Western Road, Chaoyang District-100029, Beijing, PR China.

[4]Dip.to di Scienze del Suolo, della Pianta e degli Alimenti, Università degli Studi di Bari "Aldo Moro", Via G. Amendola 165/A, 70126 BARI –Italy.

[5]Scottish Universities Environmental Research Centre, Rankine Avenue, Scottish Enterprise Technology Park, East Kilbride, G75 0QF, UK.

[*]Corresponding author: Phone: +8618322560509. E-mail: mostofa@tju.edu.cn

https://doi.org/10.5194/bg-2020-145
Preprint. Discussion started: 20 May 2020

Biogeosciences Discussions

Abstract

The production of fluorescent dissolved organic matter (FDOM) produced from phytoplankton and its subsequent degradation both of which occur constantly under diurnal-day time sunlight and by night time dark-microbial processes, influence markedly several biogeochemical processes and functions in aquatic environments and can be feasibly related to global warming (GW). In this work sunlight-mediated high-temperature was shown to accelerate the production of FDOM, but also its complete disappearance over a 24-h diurnal period in July, but not in lower temperature months. In July, extracellular polymeric substances (EPS), an early-state DOM, were produced from phytoplankton in early morning (6:00-9:00), then were degraded into four FDOM components over midday (10:00-15:00), which was followed by simultaneous production and almost complete degradation of FDOM with reformation of EPS during night time (2:00-6:00). Such transformations occurred simultaneously with the fluctuating production of nutrients (NH_4^+, NO_3^-, NO_2^-, PO_4^{3-} and dissolved Si), dissolved organic carbon (DOC), dissolved organic nitrogen (DON) and the two isotopes ($\delta^{15}N$ and $\delta^{18}O$) of NO_3^-. The FDOM components identified by fluorescence excitation-emission matrix (EEM) spectroscopy combined with parallel factor (PARAFAC) analysis consisted of EPS, autochthonous humic-like substances (AHLS) of C and M types distinctly, a combined form of C and M types of AHLS, protein-like substances (PLS), newly-released PLS, tryptophan-like substances (TLS), tyrosine-like substances (TYLS), a combined form of TYLS and phenylalanine-like substances (PALS), as well as their degradation products. Finally, stepwise degradation and production processes are synthesized in a pathway for FDOM components production and their subsequent transformation under different diurnal temperature conditions, which provided a broader paradigm for future impacts on GW-mediated DOM dynamics in lake water.

https://doi.org/10.5194/bg-2020-145
Preprint. Discussion started: 20 May 2020

Keywords: Fluorescent dissolved organic matter (FDOM); sunlight-mediated processes; dark-mediated microbial processes; transformation of FDOM; water samples; closed lakes

1. Introduction

Natural organic matter (NOM) is a key material in sustaining all biogeochemical processes and phenomena in the ecosystem. NOM originates from two primary sources, *i.e*. plant materials in terrestrial ecosystems and phytoplankton in aquatic systems. Terrestrial NOM, including soil humic substances (humic acid and fulvic acid) (Tadini et al., 2017; Senesi and Loffredo, 1999), can produce dissolved organic matter (DOM) that partially runs-off into surrounding aquatic environments (Zark and Dittmar, 2018; Mostofa et al., 2019). Conversely, autochthonous aquatic DOM includes extracellular polymeric substances (EPS), autochthonous humic-like substances (AHLS), protein-like substances (PLS), aromatic amino acids of various nature, etc (Shammi et al. 2017a, 2017b, 2017c; Guidi et al., 2016; Zhang et al., 2009; Mostofa et al. 2013; Yamashita and Tanoue, 2003). These substances occur as major fractions, even if very diluted, in surface waters of lakes, estuaries and oceans[7], thus they control many important biogeochemical functions and processes in aquatic systems, including cycling of C (Zark and Dittmar, 2018; Guidi et al., 2016; Amon and Benner, 1994), N (Yue et al., 2018; Liang et al. 2019), P (Guidi et al., 2016; Carpenter et al., 1998; Parsons et al., 2017) and trace elements (Wan et al., 2019; Helms et al., 2013), as well as nutrient changes associated with diurnal sunlight-induced planktonic photosynthesis (Gao et al., 2010; Jung et al., 2013; Segschneider and Bendtsen., 2013).

Most key DOM components of both terrestrial and aquatic autochthonous sources display fluorescence properties, thus are termed fluorescent DOM (FDOM) and can be studied in detail by fluorescence excitation-emission matrix (EEM) spectroscopy combined with parallel factor (PARAFAC) analysis (Mostofa et al., 2019; Coble, 2007; Stedmon et al., 2003; Coble, 1996). Natural sunlight is the key driving force for the production of DOM and FDOM components by photosynthesis (Gao et al., 2010; Segschneider and Bendtsen., 2013), as well as for their photoinduced degradation in sunlit surface water (Moran et al., 2000; Cory et al., 2007; Mostofa et al., 2007; Hansen et al., 2016; Stedmon et al., 2007; Ward et al., 2013). Subsequent processes

https://doi.org/10.5194/bg-2020-145
Preprint. Discussion started: 20 May 2020

typically convert high molecular weight (HMW) DOM into low molecular weight (LMW) DOM by producing hydroxyl radical ($^{\bullet}OH$) from either the photo-Fenton reaction or direct dissociation of H_2O_2 in sunlit surface waters (Vione et al., 2006; Catalán et al., 2016; Mostofa and Sakugawa, 2009; Mostofa and Sakugawa, 2016; Zhu and Kieber, 2018; Gligorovski et al., 2015). The action of microorganisms represents another key microbial degradation process that can alter DOM composition at night, *i.e.* in the absence of sunlight in both surface and deep water layers (Amon and Benner, 1994; Moran et al., 2000; Hansen et al., 2016; Diaz et al., 2013; Amon and Benner, 1996; Mostofa et al., 2005; Ma and Green, 2004).

The global warming (GW) phenomenon is ascertained to cause an increase of ambient temperature as well as an extension of the summer season (Huisman et al., 2006), which are expected to induce greater water stratification with major potential implications in aquatic environments (Watanabe et al., 2011; Hoegh-Guldberg et al. 2019; Rogelj et al., 2019; Marañón et al., 2018). Although the Paris climate agreement has set Intended Nationally Determined Contributions designed collectively to lower greenhouse gas emissions, a median warming of 2.6–3.1°C is expected by 2100 (Rogelj et al., 2016). The GW effect appears to lead to more frequent and intense heatwaves that are predicted to increase the minimum mortality temperature (Qian et al., 2019) and the risk of severe and, in some cases, irreversible impact on ecosystems (Pachauri et al., 2014; Wernberg, 2016; Frölicher et al., 2018). The frequency of sunlight-mediated high temperatures, which is clearly interconnected with the effects of GW in increasing the overall ambient temperature, is thus reasonably expected to accelerate DOM degradation, as well as all photochemical, microbial and physical processes in aquatic environments (Segschneider and Bendtsen., 2013).

Diurnal day-time (sunlight) and night-time (microbial) degradation processes are a natural phenomenon that is ultimately related to daily biogeochemical changes of C, N and P cycling, and depend on the photosynthetic activity of primary producers in surface waters (Guidi et al., 2016; Segschneider and Bendtsen., 2013; Huisman et al., 2006; Carpenter et al., 1998). Photoinduced degradation of FDOM is usually observed in the euphotic zone, especially in the summer season (Mostofa et al., 2005; Borisover et al., 2009), with a significant decrease of its fluorescence intensity with increasing water depth. Such overall day-night degradation of FDOM is caused from diurnal photo-microbial transformation. Between the years 2006 and 2015 the ambient air mean

https://doi.org/10.5194/bg-2020-145
Preprint. Discussion started: 20 May 2020

temperature has increased by about 0.94 °C in Northwest China and 1.59 °C in Northeast-North China, compared to GW values estimated at 1.5-2.0 °C (Qian et al., 2019). Currently, it is still uncertain how increasing temperature-driven trends may impact diurnal photo-microbial transformation of FDOM in freshwater lakes under GW scenarios. In any case, it is difficult to assess the potential impact of sunlight-mediated high-temperature on DOM dynamics due to the complexity of the various environmental parameters acting together.

The aim of this work was to investigate the diurnal daytime-photoinduced production of FDOM components and their associated cascade night-time-microbial degradation processes as affected by temperature in two closed lake systems. Water samples were collected along 24-h in each season from the lakes Jingye and Qingnian in China, on which water temperature, solar intensity (SI), dissolved organic carbon (DOC), dissolved organic nitrogen (DON), NO_3^-, O and N isotopes of NO_3^-, NO_2^-, NH_4^+, PO_4^{3-}, dissolved silicon (DSi), pH and electrical conductivity (EC) were determined at hourly intervals together with scanning electron microscopy imaging of phytoplankton variability between day and night. Another aim of this study was to assess the variation of nutrient contents related to the production-degradation processes of FDOM occurring during the diurnal cycles under different temperature conditions. Further, on the basis based of obtained results a comprehensive four-phase model was developed to interpret the production-degradation mechanisms of FDOM, which could be useful to predict future potential GW impacts.

2. Materials

Jingye lake and Qingnian lake are closed lakes with a watershed area of approximately 29568 m^2 and 45156 m^2, respectively, both located inside the campus of Tianjin University, Tianjin, China (39°6' N, 117°10' E) (Fig. S1). There is no connecting inflowing and outflowing channel to or from the lake, and rainwater is the most important water source. The four sides of both lakes are reinforced with granite to prevent soil erosion from the surrounding terrestrial environment and for aesthetic reasons. The waterbody of Jingye lake is directly exposed to natural sunlight, due to the absence of any obstacles, *e.g.* trees or buildings, around the lake area. Differently, Qingnian lake is relatively less exposed to natural sunshine due to the presence of many big trees and buildings along its four sides and also features some small aquatic plants and sea grasses that grow in the shallows at the lake sides.

https://doi.org/10.5194/bg-2020-145
Preprint. Discussion started: 20 May 2020

Lake waters were collected on July 5 and 6, 2018, every hour over 24 h, whereas on October 12 and 13, 2018, water samples were collected every hour in day-time (6:00 – 18:00) and at two-hours intervals in night-time (20:00 – 6:00). All times are expressed as Chinese Standard Time (CST). The diurnal results measured on FDOM components in July and October samples showed that the most important changes occurred in the afternoon at around 14:00 due to day-time sunlight-induced production and degradation and at early morning before sunrise (6:00) by night-time microbial processes. Thus, water samples on May 2 and June 30, 2019, were collected only twice-a-day, i.e. in the afternoon (14:00) and early morning (6:00). Water samples from both lakes were collected also on one day in September, December, April and June.

Water samples were collected in 500 ml brown-glass bottles previously cleaned by submergence in HCl solution for 48h and subsequently rinsed first with deionized water and then three times with ultra-pure water. Finally, the water samples were filtered through 0.45-μm glass-fiber filters previously cleaned by burning for 5-h at 450 ºC in an oven and then kept in a refrigerator at 4°C until performing analyses.

3. Methods

The DOC concentration was measured in triplicate on each sample using a combustion total organic carbon (TOC) auto-sampler analyzer (OI Analytical Aurora, Model 1030W+1088, USA). A UV-VIS spectrophotometer (UV-2700, Shimadzu) was used to estimate absorption properties of chromophoric DOM (CDOM). The pH and EC were measured in the field in real time using a multi-parameter analyzer (YSL-EXO, YSI Company, USA). Microscopic images of phytoplankton were obtained by the intelligent identification and counting instrument for algae (Algacount S300-3614025). The SI data were provided by Tianjin Meteorological Agency, Tianjin, China, whereas water and air temperatures (WT and AT, respectively) were measured at 10-min intervals using a sensor-based probe thermometer (Testo 175 Q/DT01, China). The isotopes $\delta^{15}N$ and $\delta^{18}O$ of NO_3 in water samples were measured by a method described previously (Yue et al., 2018; Mcilvin and Casciotti, 2011) using four international NO_3^- standards, i.e. USGS-32, USGS-34, USGS-35 and IAEA-N3 (United States Geological Survey (USGS), USA *via* China Isotope & Radiation Corporation, Beijing, China), for calibration. Concentrations of total N (TN), NO_3^-, NO_2^-, NH_4^+, PO_4^{3-} and dissolved silicon (DSi) were measured colorimetrically using an automated

https://doi.org/10.5194/bg-2020-145
Preprint. Discussion started: 20 May 2020

continuous flow analyzer (Skalar San++ System, Skalar Analytical B.V., The Netherlands). Dissolved organic nitrogen (DON) was estimated by subtraction of NO_3^-, NO_2^- and NH_4^+ contents from the TN content. Absorption spectra were obtained between 250 nm and 750 nm at 1-nm interval with a quartz cell of 1 cm path length using a Shimadzu UV-2401PC. Ultra-pure water was simultaneously used in the reference cell as a blank.

Fluorescence EEM spectra were recorded with a fluorescence spectrophotometer (F-7000, Hitachi, Japan) according to procedures reported elsewhere (Mostofa et al., 2010; Mostofa et al., 2018). The scanning ranges were 220–400 nm for excitation at intervals of 5 nm and 280–500 nm for emission at intervals of 1 nm using a scanning speed of 1200 nm min^{-1} and 700 v. The slit width for both the excitation and emission was set at 5 nm and all EEM spectra were recorded in both excitation and emission corrected mode. Ultrapure water (18.2 MΩ.cm) was used as the blank and measured before sample analysis after every 10 samples. In some cases, water samples were diluted to avoid inner filter effects (IFE), after which the most commonly used absorbance-based approaches (Kothawala et al., 2013; Lakowicz, 2018) were applied to correct IFE in EEM measurements.

PARAFAC analysis was performed using the "N-way Toolbox for MATLAB" (Andersson and Bro., 2000). Before applying PARAFAC, EEM data were preprocessed by subtracting Rayleigh and Raman peaks along with a ultrapure water blank from experimental EEM spectra using a home-made Excel Program (Shammi et al. 2017a, 2017c; Mostofa et al., 2010). Finally, non-negative constraints were applied to the PARAFAC model. The detailed procedure followed in applying PARAFAC modelling to EEM spectra was reported elsewhere (Mostofa et al., 2010; Mostofa et al., 2018). Further, to avoid the possible production of artifacts by mixing of fluorescent components among different water samples (Mostofa et al., 2010), PARAFAC analysis was performed on selective characteristic sample (Mostofa et al., 2019). To elucidate the diurnal production and subsequent degradation of FDOM and compare day-time-sunlight effects to night-time-microbial implications, samples were grouped into five sub-diurnal samples, i.e. samples collected at: (a) early morning (6:00-9:00) subjected to almost no sunlight effects; (b) mid-day (10:00-15:00) subjected to strong sunlight effects; (c) afternoon (16:00-20:00) subjected to moderate light effects; (d) early-night (21:00-1:00) affected by mild microbial effects ; and (e) late night-early morning (2:00-6:00) affected by strong microbial activity. Based on the selective characteristic sample (Mostofa et al. 2019), the PARAFAC model was applied individually to each

https://doi.org/10.5194/bg-2020-145
Preprint. Discussion started: 20 May 2020

of the five sub-diurnal water sample groups collected in the months of July and October. The number of water samples in each group were, respectively for July and October: 12 + 12 for early morning, 18 + 18 for mid-day, 15+15 for afternoon,15 + 6 for early night, and 15 + 9 for late night-early morning.

4. Results and Discussion

4.1. Diurnal features of FDOM in Jingye and Qingnian lake waters

4.1.1. Water samples collected in July from Jingye lake

The EEM-PARAFAC results shown in Table 1 and Fig. 1 indicated that the fluorescent components in water samples collected from Jingye lake in the early morning of July 5 and 6 from were similar and consisted of EPS in a combined form of PLS showing two fluorescence peaks (T at 270/365 nm and T_{UV} at 230/365 nm) and M-type AHLS also showing two fluorescence peaks (M at 270/394 nm and A at 230/394 nm). Generally, EPS are considered an early-stage DOM that derives either from phytoplankton (Guidi et al., 2016; Zhang et al., 2009; Mostofa et al., 2013; Casareto et al., 2012) under elevated early-morning sunlight intensity (SI, from 0.19 to 1.95 MJ/m^2 for a total of 4.18 MJ/m^2) and relatively high WT (29.3-31.0 °C) and AT (28.4-38.2 °C) or from microbially activity under dark late-night early-morning conditions also at relatively high WT (29.2-29.9 °C) and lower AT (25.4-26.2 °C) (Fig. 2) (Shammi et al. 2017a, 2017c; Sheng and Yu, 2006). The EPS excreted from microorganisms were shown to be composed mainly of polysaccharides, proteins, nucleic acids, lipids and a HMW mixture of polymeric AHLS (Sheng and Yu, 2006; Flemming and Wingender, 2010; Jenkinson and Lappin-Scott, 2011).

Apparently, EPS generated at early morning were subsequently degraded during mid-day time (10:00-15:00) into four FDOM components that include: (a, b) AHLS of C and M types featuring two fluorescence peaks each, i.e. respectively C at 315/418 nm and A at 260/418 nm, and M at 305/383 nm and A at 220/383 nm); (c) TLS showing two fluorescence peaks (T at 270/338 nm and T_{UV} at 225/338 nm); and (d) newly-released PLS featuring two fluorescence peaks (C at 315/418 nm and A at 260/418 nm) (Table 1, Fig. 1). FDOM production by degradation of EPS would occur during the gradual increase of SI (from 1.36 to 2.97 MJ/m^2 for a total = 15.26

https://doi.org/10.5194/bg-2020-145
Preprint. Discussion started: 20 May 2020

225 MJ/m^2) at WT of 30.2-33.7 °C and AT of 35.4-41.8 °C (Fig. 2) (Zhang et al., 2009; Parlanti et al.,
226 2000; Yamashita and Youhei, 2004; Yamashita and Tanoue, 2003; Coble, 1996).

227 In the late-afternoon early-evening time period (16.00-20.00), a number of changes of the
228 four FDOM components occurred (Table 1, Fig. 2) under the varied conditions of SI (from 0.01 to
229 0.85 MJ/m^2 for a total of 1.77 MJ/m^2), WT (30.9-33.4 °C) and AT (29.0-38.1 °C) (Fig. 1). In
230 particular: (a) newly-released PLS with a peak T at 280/351 nm appeared; (b) the T_{UV} peak
231 disappeared; (c) the fluorescence peak C of C type-AHLS was partly shifted to longer wavelength,
232 i.e. 325/430 nm; (d) peak M of M type-AHLS showed a 3.2-fold intensity increase; and (e) the
233 fluorescence intensity of peak C and peak T of TLS decreased, respectively, by about 3% and
234 63%), whereas the intensity of peak T of newly-released PLS increased by 49%. The daytime-
235 photoinduced degradation of FDOM could be ascribed to the occurrence of photo-Fenton reaction
236 that produced the strong oxidizing agent $^{\bullet}OH$ radical by reaction of H_2O_2 and Fe^{2+} in the presence
237 of sunlight (Vione et al., 2006; Mostofa and Sakugawa, 2016; Gligorovski et al., 2015). In the
238 early-night samples, under conditions of WT (29.9-30.8 °C) and AT (26.0-28.9 °C) (Fig. 2), only
239 two FDOM components, i.e. AHLS of C type and TLS were identified with intensity increased by,
240 respectively, approximately 40% and 3.2-fold, whereas the other two fluorescent components
241 disappeared completely.

242 Finally, in the samples collected during late-night early-morning 2.00-6.00) under
243 conditions of WT (29.2-29.9 °C) and AT (25.4-26.2 °C) (Fig. 2), only EPS generated from
244 grazing/respiration of primary producers, i.e. phytoplankton were identified, whereas the other
245 fluorescent components disappeared completely. In particular, the estimated production of EPS
246 in this time period was approximately 3% lower than in early morning as shown by the microscope
247 images of phytoplankton that mostly disappeared during the day (Fig. S2). The diurnal changes of
248 FDOM components could be reasonably caused by: (a) the simultaneous photoinduced production
249 and microbial degradation under daytime conditions of high sunlight intensity and ambient
250 temperature, as also reported by previous *in situ* experimental investigations (Moran et al., 2000;
251 Mostofa et al., 2007; Mostofa et al., 2005; Ma and Green, 2004), and (b) night-time extended
252 microbial degradation, which was also supported by the net increase of dissolved inorganic carbon
253 (DIC) components comprising dissolved CO_2, H_2CO_3, HCO_3^-, and CO_3^{2-}, in water samples
254 collected at a depth of at 24 m (no light effects) with respect to that at 6.5-m depth (Ma and Green,

https://doi.org/10.5194/bg-2020-145
Preprint. Discussion started: 20 May 2020

255 2004). In conclusion, the July 2018 sampling campaign was performed at the highest AT (ranging
256 from 25.4 to 41.8 °C with an average of 31.6 °C) and WT (ranging from 29.2 to 33.7 °C with an
257 average of 31.0 °C) and a daily total solar intensity of 21.39 MJ m^{-2} (Fig. 2).

258 ***4.1.2. Water samples collected in October from Jingye lake***

259 The diurnal transformations of samples collected in October under conditions of lower sunlight
260 irradiation and lower WT and AT values were partially different from those collected in July. In
261 October, four fluorescent components were identified in water samples collected at early-morning
262 (6.00-9.00) under conditions of SI from 0.004 to 1.34 MJ/m^2 for a total of 2.29 MJ/m^2) and WT
263 ranging from 16.5 to 18.3 °C and AT from 9.4 to 14.5 °C (Fig. 2). These included AHLS of C and
264 M types, PLS and degraded TLS (Table 1, Fig. 3). In particular, PLS were identified by two
265 fluorescence peaks (T at 285/352 nm and T_{UV} at 235/352 nm), whereas the peaks of the other three
266 FDOM components were similar to those of July samples, although peak intensities varied
267 depending on sunlight-driven temperature (Table 1, Fig. 3). In particular, newly-released PLS
268 could be recognized by a major T peak and a minor T_{UV} peak which was absent and TLS that
269 showed the typical peaks T_{UV} at 220-225 nm and T at 270-280 nm with an intensity ratio of 5.2,
270 which was the key signature that distinguished TLS from PLS.

271 In the subsequent mid-day temporal interval (10.00-16.00) characterized by a SI ranging from
272 1.34 to 2.26 MJ/m^2 for a total of 11.46 MJ/m^2, WT from 18.1 to 20.6 °C and AT from 15.2 to
273 22.9 °C (Fig. 2). few variations of fluorescence peaks were detected for the four components
274 (Table 1). The peak intensity ratio (T_{UV}/T) was 1.14 for PLS and 2.72for TLS. Further, compared
275 to early-morning samples, the fluorescence intensity increased of approximately 63% for peak M
276 (HLS) and 58% for peak T (TLS) but deceased, approximately 9% for peak C of AHLS and 5%
277 for peak T of PLS.

278 The water sample collected in the afternoon-evening (16.00-20.00) under conditions of very
279 low SI (from 0.14 to 0.57 MJ/m^2 for a total of 0.71 MJ/m^2) and low WT (17.5-20.2 °C) and AT
280 (15.5-22.7 °C) showed three fluorescent components identical to those of earlier phases but PLS
281 peaks disappeared completely. The fluorescence intensity increased slightly, i.e. approximately 9%
282 for C-type AHLS and 4% for TLS, but decreased of 16% for M-type AHLS. In the following early-
283 night temporal period (21.00-1.00) under conditions of no sunlight and relatively low WT (16.8-
284 17.4 °C) and AT (14.2-15.7 °C), four fluorescent components were identified of which three were

https://doi.org/10.5194/bg-2020-145
Preprint. Discussion started: 20 May 2020

identical to those detected in the samples of previous periods and the fourth was ascribed to PLS newly-released from phytoplankton (Fig. 3). Further, fluorescence intensities decreased of approximately 23% for M-type AHLS and 4.6% for TLS, but increased of about 31% for C-type AHLS. Lastly, in the late-night early-morning period (2.00-6.00) with no sunlight and low WT (14.0-16.8 °C) and AT (13.9-14.8 °C), four fluorescent components were identified, i.e. M-type AHLS freshly generated by the disappearance of newly-released PLS, a degraded M-type AHLS, C-type AHLS and TLS, with a decreased intensity, compared to the previous period of, respectively, approximately 34%, 15% and 52% (Table 1, Fig. 3). The production of AHLS of M-type was the key signature of freshly formed DOM from newly-released PLS produced in the previous time period. Apparently, in October, the low sunlight-affected ambient temperature was not able to degrade all FDOM in a 24-h cycle and, correspondingly, EPS was not generated from phytoplankton as it occurred in July. The newly released PLS generated in early-night time suggested their possible derivation from EPS, whereas their low concentration and rapid subsequent transformation into other FDOM components would support their absence in water samples collected in October.

4.1.3. Water samples collected in May and June from Jingye lake

Three FDOM components were identified in water samples collected in May in the 6.00-14.00 time interval under conditions of SI of 20.47 MJ/m^2, WT from 19.2 to 26.9 °C with an average of 22.4 °C and AT from 17.1 to 35.3 °C with an average of 26.0 °C. These included AHLS of C and M types and TLS, whose fluorescence peak wavelengths were similar to those previously described (Table 2). Compared to samples collected at 6.00, the peak intensity increased for samples collected at 14.00 of approximately 36% for C-Type AHLS and 14% for TLS, but decreased by 95% for M-Type AHLS. These results suggested that M-Type AHLS degraded rapidly by sunlight-induced photoprocesses, whereas the other two FDOM components could regenerate from phytoplankton by photorespiration. The new production of C-Type AHLS was supported by the longer emission wavelength of peak C, i.e. 340/468 nm, measured at 14:00 with respect to that at 6:00, i.e. 340/449 nm) (Table 2).

Also in June, three FDOM components, i.e. AHLS of C and M types and TLS, were identified in the early morning (6:00) samples, whereas in the early afternoon samples (14.00), besides the typical C-type AHLS and TLS, a degraded EPS featuring four fluorescence peaks was detected,

https://doi.org/10.5194/bg-2020-145
Preprint. Discussion started: 20 May 2020

315 which included a combined form of C and M types of AHLS, whose wavelengths were shifted to
316 longer values than in July, with disappearance of any PLS contribution (Table 2, Fig. 5). The
317 FDOM transformations described above occurred under conditions of SI of 21.18 MJ/m^2, WT
318 ranging from 27.5 to 33.9 °C with an average of 29.7 °C and AT ranging from 24.7 to 39.9 °C
319 with an average of 30.4 °C. Apparently, the overall night-time FDOM microbial production was
320 altered in the early morning (6:00) with subsequent production of new FDOM components under
321 the strong day-time sunlight effect until 14.00. Thus, the increased sunlight-mediated ambient
322 high-temperature under GW conditions could be expected to accelerate FDOM production with
323 transformation into LMW DOM within the 24-h period as observed in July but not in lower
324 temperature months.

325 ***4.1.4. Water samples collected in May and June from Qingnian lake***

326 Differently from Jingye lake, four fluorescent components were identified in May in
327 Qingnian lake waters at both 6:00 and 14:00, which included, besides C and M types of AHLS and
328 TLS, new components, i.e. TYLS and PALS, which were previously detected in surface waters by
329 other means (Yamashita and Tanoue, 2003, Mostofa et al., 2018). In particular, partially degraded
330 TYLS were detected at 6:00 featuring only one fluorescence peak (T_{UV} at 220/313 nm), whereas
331 at 14:00 a combined form of TYLS and PALS showing two fluorescence peaks (T at
332 255,265/321,306,310 nm and T_{UV} at 220/321 nm) were detected (Table 2, Fig. 4). The occurrence
333 of peak T with two excitation maxima and three emission maxima suggested the existence of a
334 combined state of TYLS and PALS that could originate from EPS, which were detected for the
335 first time in this work, so adding new information on the sequential formation of two aromatic
336 amino acids in a combined state under current lake environmental conditions. The fluorescence
337 intensity of C-type AHLS remained almost constant (2% decrease), whereas those of M-type
338 AHLS and TLS increased, respectively, by approximately 4% and 30% at 14:00 compared to the
339 values measured at 6:00. The production and degradation processes of FDOM described above
340 occurred at a SI of 20.47 MJ/m^2, a WT between 19.5 and 23.4 °C with an average of 21.5 °C and
341 AT between 17.6 and 38.7 °C with an average of 26.2 °C (Fig. 2).

342 Similarly, four FDOM components were identified in June at both 6:00 and 14:00, which
343 included C and M types of AHLS, newly-released PLS (6:00) or PLS (14:00) and TLS (Table 2,
344 Fig. 4). The newly-released PLS present in waters collected at early morning (6.00) were identified

https://doi.org/10.5194/bg-2020-145
Preprint. Discussion started: 20 May 2020

by two fluorescence peaks, i.e. a major peak T at 290/346 nm of significantly high fluorescence intensity and minor peak T_{UV} at 230/346 nm. Apparently, the newly-released PLS detected at early morning (6:00) would convert into different PLS detected at 14.00, which featured two fluorescence peaks (T at 285/340 nm and T_{UV} at 225/340 nm). During the 6.00 to 14.00 time period the fluorescence intensity of the C-type AHLS decreased approximately of 26%, whereas those of M-type AHLS and TLS increased, respectively, by 43% and 16%. These FDOM modifications occurred at a SI of 21.18 MJ/m^2, a WT between 26.9 and 36.8 °C with an average of 30.4 °C and an AT between 23.6 and 41.5 °C with an average of 30.5 °C (Fig. 2). The detection of newly-released PLS in June in the early morning (6:00) was a key signature indicating a fresh input from EPS under conditions of enhanced WT that could have occurred during the night-time due to microbial respiration. However, such scenarios were not observed in this lake in May when WT was significantly lower than in June (Fig. 2). With respect to May, the overall fluorescence intensity in June at 14.00 decreased by approximately 39% for C-type AHLS and 40% for TLS, but that of M-type AHLS increased of 47%, which indicated that FDOM production-degradation dynamics varied significantly on dependence on sunlight-mediated ambient temperature.

4.1.5. Seasonal characteristics of FDOM and their transformation in the two lakes

The fluorescent components in Jingye lake water varied significantly between the four seasons (Table S1, Fig. S3). In particular, in autumn three FDOM components were identified including AHLS (C and M types) and PLS (Fig. S3), whereas four FDOM were identified in the other three seasons, of which the first two was similar in all seasons. A third component was identified as newly-released PLS featuring two fluorescence peaks, a major one (T at 285/369 nm) and a minor one (T_{UV} at 250/369 nm) in samples collected in spring, and only one peak (T at 285/354 nm) in summer sample. The fourth component was identified as TLS These results indicated that C and M types AHLS were detected in all seasons, whereas the major changes in FDOM could be attributed to proteinaceous components, i.e. PLS, and their transformation products, i.e. individual aromatic amino acids including TLS, TYLS and PALS.

The FDOM components in Qingnian lake waters also changed substantially as a function of the season. In detail: (a) two components, i.e. M-type AHLS and a unkown degraded component in autumn; (b) one component, i.e. EPS as a combined form of HLS and PLS with four fluorescence peaks, in winter; (c) two components, i.e. C-type AHLS and TLS in spring; and (d)

https://doi.org/10.5194/bg-2020-145
Preprint. Discussion started: 20 May 2020

four components, i.e. C and M types AHLS, newly-released PLS and TLS in summer (Table S1, Fig. S4). These results suggested that at low winter temperatures EPS could be produced in lake water and that the seasonal production of FDOM and its biogeochemical transformations differed between the two lakes, which could be ascribed to the different lake conditions and surrounding environmental factors.

4.2. Biogeochemical processes involving DOC and nutrients in lake Jingye

In July, DOC concentration varied hourly from a minimum of 815 μM C achieved in the night (from 21.00 to 6.00) to a maximum of 963 μM C reached during the day (from 10.00 to 16.00), with the highest DOC fluctuation of 18% (Table S2, Fig. 6). In October, the DOC content was generally higher than in July and varied from low night values with a minimum of 975 μM C at early morning (6:00) to a maximum of 2989 μM C during the day-time (10.00-15.00) with an increase of approximately 3.07-fold at 14:00 (Table S2, Fig. 6). The trends of DOC concentration were paralleled by those of nutrients which in October were generally higher and more fluctuating along the day than in July (Table S2, Fig. 6). In particular, in July the NO_3^- content decreased of about 20% from early morning (6.00-9.00), to middle day (10.00-15.00) and subsequently increased (1.0-7.8%) in all successive sub-diurnal samples, whereas in October, it increased of about 10.0% during morning from 6 to 15.00, then remained nearly constant and increased again of about 16.0% during night time (2.00-6.00). Differently, NO_2^- increased substantially (70.0-94%) during day-time in October compared to July (0.5-14.4%), but then decreased significantly (5.0-5.8%) during night-time, which suggested a rapid turnover rate of NO_2^- during phytoplankton growth. Similarly, NH_4^+ substantially increased in October (117.0-257.0%) compared to the same time interval in July (4.1-41.7%), with the highest increase in the middle of the day (10.00-15.00). The DON content increased (7.6-31.0%) between 6.00-9.00 in July, whereas it was not detected in samples collected in October. The PO_4^{3-} content decreased significantly in July during the 16.00-20.00 period and then increased (18.0-34%) in night-time, whereas in October it decreased (11.4-40.0%) in night- time, showing the highest concentrations in the 16.00-20.00 time period. In July, DSi decreased (3-17%) from early morning (6:00-9:00) to late day, with an early night (21.00-1.00) increase of 23%, whereas it was absent in samples collected in October, which suggested its complete uptake by phytoplankton during the strong growth period occurring in this month.

https://doi.org/10.5194/bg-2020-145
Preprint. Discussion started: 20 May 2020

405 The highest production of nutrients in October than in July was estimated to be
406 approximately of 16.0, 28, 4.0 and 23.8-fold respectively for NO_3^-, NO_2^-, NH_4^+, and PO_4^{3-} (Fig.
407 6). In particular, in October the highest NH_4^+ concentration paralleled the highest DOC
408 concentration detected at the same time (14.00) (Table S2, Fig. 6), which suggested a rapid
409 biogeochemical transformation of organic matter into DOC and nutrients under ambient lake
410 conditions. Apparently, the NH_4^+ formation in October was followed by its subsequent rapid
411 nitrification and denitrification at same time (14.00) (Table S2, Fig. 6). Similarly, the lowest level
412 of NH_4^+ at 10.00 was consistent with the lowest level of NO_3^-. Further, the occurrence of
413 nitrification was confirmed by the decrease of NH_4^+ contents occurring simultaneously to the
414 increase of NO_3^- in early morning samples (Table S2, Fig. 6).

415 Further evidence of photoinduced respiration of phytoplankton was provided by the
416 significant shifting of the $\delta^{15}N$ value of NO_3^-. In particular, in July the $\delta^{15}N$ value decreased from
417 +0.67‰ at 10:00 to −0.02‰ at 12:00, which corresponded to the increase of SI from 2.33 MJ m^{-2}
418 to 2.95 MJ m^{-2} (for a total of 8.14 MJ m^{-2}), whereas the $\delta^{18}O$ value of NO_3^- increased from +5.28‰
419 at 10:00 to +9.3‰ at 12:00 under conditions of elevated SI and high WT (36.5-39.9 °C) and AT
420 (31.0-32.7 °C). The decrease of $\delta^{15}N$ and increase of $\delta^{18}O$ in NO_3^- with increasing SI from 10:00
421 to 12:00 indicated the uptake of lighter $\delta^{16}O$-containing NO_3^- by phytoplankton with increasing
422 photosynthesis. This effect was confirmed by the 20% decrease of NO_3^- from 9:00 to15:00 in July,
423 whereas in samples collected in October the disappearance of DSi with the corresponding high
424 production of DOC and nutrients would indicate the occurrences of high photosynthetic activity
425 with a high production of phytoplankton during day-time from both photoinduced processes and
426 microbial respiration of planktonic organisms, which confirmed earlier results (Fan and Glibert,
427 2005; Guidi et al. 2016; Parsons et al. 2017; Condon et al. 2010; Carpenter et all. 1998; Elser et al.
428 1995). Thus, the activity of photosynthetic planktonic communities in sunlit surface water with
429 the simultaneous release of DOC and nutrients could represent the driving force of the overall
430 biogeochemical processes and functions occurring in surface lake waters.

431

432 ***4.3. A global view of production and degradation pathways of FDOM in lake waters***

433 As the different components of FDOM are related each to the other, their sequential
434 derivation/origin from phytoplankton and their subsequent transformation steps can be illustrated

https://doi.org/10.5194/bg-2020-145
Preprint. Discussion started: 20 May 2020

435 in the pathway shown in Fig. 7 and detailed in Figs. 12 and 13. In particular, in the first step
436 primary DOM producers, mainly phytoplankton, generate EPS that in the second step produce
437 FDOM components of various nature, which in the third step are subject to simultaneous
438 subsequent stepwise degradation and production processes that follow two major distinct and
439 parallel pathways. On the basis of results described and discussed above, these pathways can be
440 reasonably hypothesized to consist of: (a) EPS are firstly transformed into a combined form of
441 AHLS of C and M types, which are commonly detected in surface waters (Shammi et al. 2017a,
442 2017b, 2017c; Sheng, G. P.; Yu, 2006; Sheng et al. 2010), then these convert into degraded forms
443 that finally yield LMW DOM and mineralized end-products (Fig. 8); and (b) EPS are converted
444 into newly-released PLS that subsequently generate PLS and individual TLS, TYLS and PALS,
445 which have been detected previously in surface water exposed to sunlight (Mostofa et al., 2019;
446 Zhang et al., 2009; Mostofa et al. 2013; Shammi et al. 2017a, 2017b, 2017c; Yamashita and Tanoue,
447 2003; Mostofa et al. 2010), that finally degrade to LMW DOM and mineralized end-products (Fig.
448 9). Further, in the last step, as well as in all previous steps, mineralized end-products, including
449 nutrients, CO_2, DIC, H_2O_2, etc., are continuously produced both under diurnal sunlight-induced
450 degradation and night-time microbial degradation.

451 In more detail, the currently undefined formation of EPS in the first step of the process
452 described above has been proved to occur mainly in July in early-morning (from 6.00 to 9.00),
453 which is indicative of its production under the effect of sunlight-induced, high-temperature, day-
454 time microbial respiration, whereas their subsequent degradation into various FDOM components
455 would occur during intense sunlight period (from 10.00 to 15.00), which is followed by
456 simultaneous production-degradation processes taking place during relatively low sunlight effect
457 (from 16.00 to 20.00), after which FDOM is degraded almost completely during the night (from
458 21.00 to 6.00). Differently, only partial transformations of FDOM components are measured in
459 water samples collected in the other months due to the lower solar intensity and water and air
460 temperatures with respect to July. Although an accurate calculation of the net production-
461 degradation of FDOM components is very difficult due to the simultaneous occurrence of these
462 processes under either photo-respiration in day-time or microbial respiration in night-time, the net
463 diurnal changes of fluorescence intensities calculated as a function of the time, which have been
464 discussed in detail in the previous section, can provide a good quantitative approximation of these
465 processes.

https://doi.org/10.5194/bg-2020-145
Preprint. Discussion started: 20 May 2020

5. *Conclusions*

It is well-known that phytoplankton releases continuously EPS and, in turn, FDOM due to both photoinduced processes and microbial-respiration (Wang et al., 2017; Shammi et al. 2017a, 2017b, 2017c; Guidi et al., 2016; Parlanti et al., 2000; Zhang et al., 2009; Mostofa et al. 2013; Yamashita and Youhei, 2004), which is then subject to continuous sunlight-induced degradation in the upper sunlit surface waters (from 0 to about 5 m and even more deeply) and by microbial degradation in deeper-layer waters (Amon and Benner, 1994; Moran et al., 2000; Mostofa et al., 2007; Diaz et al., 2013; Amon and Benner, 1996; Mostofa et al., 2005). Although photoinduced degradation has been proved to be mediated by $^{\bullet}OH$ radicals generated from photo-Fenton reaction or direct dissociation of H_2O_2 under sunlit surface waters (Wang et al., 2017; Vione et al., 2006; Mostofa and Sakugawa, 2009; Mostofa and Sakugawa, 2016; Zhu and Kieber, 2018; Gligorovski et al., 2015), the diurnal transformation mechanisms of complex mixtures of FDOM of diverse composition existing in surface waters are not yet well understood.

In this work the existence in lake waters of different types of autochthonous FDOM that can be produced by phytoplankton, which include EPS, AHLS of C and M types, PLS, newly-released PLS, TLS, a combined form of C and M types of AHLS, a combined form of TYLS and PALS, as well as their degradation products have been ascertained. The generation of different FDOM components appears to be strictly related to various factors including sunlight-mediated temperature, seasonal temperature, timescale, type and nature of primary producers, *e.g.* phytoplankton, as well as lake conditions and ambient environment. Further, on dependence on these environmental factors and conditions, the sequential production of FDOM and its subsequent degradation result to occur rapidly even in the one-day timeframe.

The information provided in this paper on the continuous production and concurrent degradation processes of FDOM in the aquatic environment are crucial for predicting and evaluating their intensification in the future due to the expected extended summer season with increased air and water temperatures and increased water stratification, as a consequence of the ascertained GW implications. Further, the information presented on the end-products of these processes appear to be of ultimate impact for a better understanding of trophic levels and most other biogeochemical processes and functions, including the sustainability of microbial food web and C, N and other nutrient cycling, occurring in aquatic ecosystems as a whole.

https://doi.org/10.5194/bg-2020-145
Preprint. Discussion started: 20 May 2020

Author contributions

K.M.G.M. designed the study. Y.L., M.M., X.Y., X.L. and L.L. performed field work, sample preparation, and EEM measurement. Y.L. performed nutrients and other measurements. Y.L. and J.Y. performed PARAFAC analysis. F.-J.Y. and S.L. performed dual NO_3^- isotopes measurement. B.W. performed microscopic phytoplankton measurement. R.M.E., C.Q.L. and S.L. revised the manuscript. K.M.G.M., N.S. and Y.L. wrote the manuscript.

ACKNOWLEDGMENTS

This work was financially supported by the National Key R & D Program of China (2016YFA0601000) and National Natural Science Foundation of China (U1612441) and also by the Key Construction Program of the National "985" Project, Tianjin University, China.

Notes

The authors declare no competing financial interest.

References

Amon, R. M. W. and Benner, R.: Rapid cycling of high-molecular-weight dissolved organic matter in the ocean, Nature, 369 (6481), 549-552, 1994.

Amon, R. M. W. and Benner, R.: Photochemical and microbial consumption of dissolved organic carbon and dissolved oxygen in the Amazon River system, Geochim. Cosmochim. Acta, 60 (10), 1783-1792, 1996.

Andersson, C. A. and Bro, R.: The N-way toolbox for MATLAB, Chemom. Intel. Lab. Syst., 52 (1), 1-4, 2000.

Borisover, M., Laor, Y., Parparov, A., Bukhanovsky, N. and Lado, M.: Spatial and seasonal patterns of fluorescent organic matter in Lake Kinneret (Sea of Galilee) and its catchment basin, Water Res., 43 (12), 3104-3116, 2009.

Carpenter, S. R., Cole, J. J., Kitchell, J. F. and Pace, M. L.: Impact of dissolved organic carbon, phosphorus, and grazing on phytoplankton biomass and production in experimental lakes, Limnol. Oceanogr., 43, (1), 73-80, 1998.

Catalán, N., Marcé, R., Kothawala, D. N. and Tranvik, L. J.: Organic carbon decomposition rates controlled by water retention time across inland waters. Nat. Geosci., 9 (7), 501-504,2016.

Coble, P., G.: Characterization of marine and terrestrial DOM in seawater using excitation−emission matrix spectroscopy, Mar. Chem., 51 (4), 325-346, 1996.

https://doi.org/10.5194/bg-2020-145
Preprint. Discussion started: 20 May 2020

527 Coble, P. G.: Marine optical biogeochemistry: the chemistry of ocean color. Chem. Rev., 38 (20),
528 402-418, 2007.
529 Condon, R. H., Steinberg, D. K. and Bronk, D.: Production of dissolved organic matter and
530 inorganic nutrients by gelatinous zooplankton in the York River estuary, Chesapeake Bay, J.
531 Plankton Res. 32(2), 153-170, 2010.
532 Cory, R. M., McKnight, D. M., Chin, Y.-P., Miller, P. and Jaros, C. L.: Chemical characteristics
533 of fulvic acids from Arctic surface waters: Microbial contributions and photochemical
534 transformations, Geophys. Res., 2007, 112 (G4), G04S51, 2007.
535 Diaz, J. M., Hansel, C. M., Voelker, B. M., Mendes, C. M., Andeer, P. F. and Tong, Z.: Widespread
536 production of extracellular superoxide by heterotrophic bacteria, Science, 340 (6137), 1223-
537 1226, 2013.
538 Elser, J. J., Chrzanowski, T. H., Sterner, R. W., Schampel, J. H. and Foster, J. H.: Elemental ratios
539 and the uptake and release of nutrients by phytoplankton and bacteria in three lakes of the
540 Canadian shield, Microb. Ecol., 29, 145–162, 1995.
541 Flemming, H. C. and Wingender, J.: The biofilm matrix, Nat. Rev. Microbiol., 8 (9), 623-633,
542 2010.
543 Frölicher, T. L., Fischer, E. M. and Gruber, N., Marine heatwaves under global warming, Nature,
544 2018, 560 (7718), 360-364, 2018.
545 Gao, K. L., Ping, Watanabe, T. and Walter Helbling, E., Combined effects of ultraviolet radiation
546 and temperature on morphology, photosynthesis, and DNA of arthrospira (*spirulina*) platensis
547 (*cyanophyta*), Phycology, 44 (3), 777-786, 2010.
548 Gligorovski, S., Strekowski, R., Barbati, S. and Vione, D.: Environmental Implications of
549 Hydroxyl Radicals (center dot OH), Chem. Rev., 115 (24), 13051-13092, 2015.
550 Guidi, L., Chaffron, S., Bittner, L., Eveillard, D., Larhlimi, A., Roux, S., Darzi, Y., Audic, S.,
551 Berline, L. and Brum, J.: Plankton networks driving carbon export in the oligotrophic ocean,
552 Nature, 532 (7600), 465-470, 2016.
553 Hansen, A., Kraus, T. E. C., Pellerin, B. A., Fleck, J. A. and Bergamaschi, B. A.: Optical properties
554 of dissolved organic matter (DOM): Effects of biological and photolytic degradation, Limnol.
555 Oceanogr., 61 (3), 1015-1032, 2016.
556 Helms, J. R., Mao, J., Schmidtrohr, K., Abdulla, H. and Mopper, K., Photochemical flocculation
557 of terrestrial dissolved organic matter and iron, Geochim. Cosmochim. Acta, 121 (6), 398-
558 413, 2013.
559 Hoegh-Guldberg, O., Jacob, D., Taylor, M. et al.: The human imperative of stabilizing global
560 climate change at 1.5°C, Science, 365, eaaw6974, 2019.
561 Huisman J., Thi, N. N., Pham, Karl, D. M. and Ben, S.: Reduced mixing generates oscillations and
562 chaos in the oceanic deep chlorophyll maximum., Nature, 439, (7074), 322-325, 2006.
563 Jenkinson, H. F. and Lappin-Scott, H. M.: Biofilms adhere to stay, Trends Microbiol., 9 (1), 9-10,
564 2001.
565 Jung, S. W., Youn, S. J., Shin, H. H., Yun, S. M., Ki, J. S. and Jin, H. L.: Effect of temperature on
566 changes in size and morphology of the marine diatom, Ditylum brightwellii (West) Grunow
567 (*Bacillariophyceae*). Estuar. Coast. Shelf Sci., 135 (135), 128-136, 2013.
568 Kothawala, D. N., Murphy, K. R., Stedmon, C. A., Weyhenmeyer, G. A. and Tranvik, L. J., Inner
569 filter correction of dissolved organic matter fluorescence. Limnol. Oceanogr.-Methods, 11,
570 616-630, 2013.
571 Lakowicz, J. R.: Plasmonics in biology and plasmon-controlled fluorescence. Plasmonics, 1 (1),
572 5-33, 2006.

https://doi.org/10.5194/bg-2020-145
Preprint. Discussion started: 20 May 2020

Liang. X. et. al., Control of the hydraulic load on nitrous oxide emissions from cascade reservoirs, Environ. Sci. Technol., 53, 11745−11754, 2019

Ma, X. and Green, S. A.: Photochemical Transformation of Dissolved Organic Carbon in Lake Superior—An In-situ Experiment, Great Lakes Res., 30, (04), 97-112, 2004.

Marañón, E., Lorenzo, M. P., Cermeño, P. and Mouriñocarballido, B.: Nutrient limitation suppresses the temperature dependence of phytoplankton metabolic rates. The ISME J., 12 (7), 1836-1845, 2018.

Mcilvin, M. R. and Casciotti, K. L.: Technical updates to the bacterial method for nitrate isotopic analyses, Anal. Chem., 83 (5), 1850-1856, 2011.

Mohinuzzaman, M., Yuan, J., Yang, X., Senesi, N., Mostofa, K. M. G. and Liu, C. Q.: Insights into solubility of soil humic substances and their fluorescence characterisation in three characteristic soils, Sci. Total Environ. 720, 137395, 2020.

Moran, M. A., Sheldon W. and Zepp R.G.: Carbon loss and optical property changes during long-term photochemical and biological degradation of estuarine dissolved organic matter, Limnol. Oceanogr., 45 (6), 1254-1264, 2000.

Mostofa, K. M. G., Yoshioka, T., Konohira, E., Tanoue, E., Hayakawa, K. and Takahashi, M.: Three-dimensional fluorescence as a tool for investigating the dynamics of dissolved organic matter in the Lake Biwa watershed, Limnology, 6 (2), 101-115, 2005.

Mostofa, K. M. G., Yoshioka, T., Konohira, E. and Tanoue, E.: Photodegradation of fluorescent dissolved organic matter in river waters, Geochem. J., 41 (5), 323-331, 2007.

Mostofa, K. M. G., Wu, F., Liu, C. Q., Fang, W. L., Jie, Y., Ying, W. L., Li, W. and Mei, Y.: Characterization of Nanming River (southwestern China) sewerage-impacted pollution using an excitation-emission matrix and PARAFAC, Limnology, 11 (3), 217-231, 2010.

Mostofa, K. M. G. and Sakugawa, H.: Spatial and temporal variations and factors controlling the concentrations of hydrogen peroxide and organic peroxides in rivers, Environ. Chem., 6 (6), 524-534, 2009.

Mostofa, K. M. G., Yoshioka, T., Mottaleb, A., and Vione, D. (Eds.): Photobiogeochemistry of Organic Matter: Principles and Practices in Water Environments, in: Environmental Science, Springer, Berlin, Heidelberg, 2013.

Mostofa, K. M. G. and Sakugawa, H.: Simultaneous photoinduced generation of Fe^{2+} and H_2O_2 in rivers: An indicator for photo-Fenton reaction, J. Environ. Sci., 47, 34-38, 2016.

Mostofa, K. M. G., Li, W., Wu, F., Liu, C.-Q., Liao, H., Zeng, L. and Xiao, M.: Environmental characteristics and changes of sediment pore water dissolved organic matter in four Chinese lakes, Environ. Sci. Pollut. Res., 25, 2783–2804, 2018.

Mostofa, K. M. G., Jie, Y., Sakugawa, H. and Liu, C.-Q.: Equal treatment of different EEM data on PARAFAC modeling produces artifact fluorescent components that have misleading biogeochemical consequences, Environ. Sci. Technol., 53 (2), 561-563, 2019.

Parlanti, E.: Dissolved organic matter fluorescence spectroscopy as a tool to estimate biological activity in a coastal zone submitted to anthropogenic inputs, Org. Geochem., 31 (12), 1765-1781, 2000.

Parsons, C.T., Rezanezhad, P. F., O'Connell, D. W. and Van Cappellen, P.: Sediment phosphorus speciation and mobility under dynamic redox conditions. Biogeosciences, 14, 3585–3602, 2017.

Qian, Y., Wang, J., Ren, Z., Li, J. and Guo, Y.: Mapping the increased minimum mortality temperatures in the context of global climate change. Nat. Commun., (10), 4640, 2019.

Rogelj, J., Huppmann, D., Krey, V., Riahi, K., Clarke, L., Gidden, M., Nicholls, Z. and

https://doi.org/10.5194/bg-2020-145
Preprint. Discussion started: 20 May 2020

Meinshausen, M.: A new scenario logic for the Paris Agreement long-term temperature goal, Nature, 573 (7774), 357-363, 2019.

Segschneider, J. and Bendtsen, J.: Temperature-dependent remineralization in a warming ocean increases surface pCO_2 through changes in marine ecosystem composition, Glob. Biogeochem. Cyc., 27 (4), 1214-1225, 2013.

Senesi, N. and Loffredo, E.: The Chemistry of Soil Organic Matter, in: Sparks, D.L. (Ed.), Soil Physical Chemistry. CRC Press, Boca Raton, pp. 239–370, 1999.

Shammi M., P. X., Mostofa KMG, Zhang D and Liu CQ, Photo−flocculation of algal biofilm extracellular polymeric substances and its transformation into transparent exopolymer particles: Chemical and spectroscopic evidences, Sci. Rep., 7, 9074, 2017a.

Shammi, M., Pan, X., Mostofa, K. M. G., Zhang, D., Liu, C.-Q. and Song, W.: Investigating extracellular polymeric substances from microbial mat upon exposure to sunlight. Poly. Degrad. Stabil., 146, 192-200, 2017b.

Shammi, M., Pan, X., Mostofa, K. M. G., Zhang, D. and Liu, C. Q.: Seasonal variations and characteristics differences in the fluorescent components of extracellular polymeric substances from mixed biofilms in saline lake, Sci. Bull., 62 (62), 764-766, 2017c.

Casareto, B. E., Niraula, M. P. and Suzuki, Y.: Dynamics of organic carbon under different inorganic nitrogen levels and phytoplankton composition, Estuar. Coast. Shelf Sci., 102-103 (5), 84-94, 2012.

Sheng, G. P. and Yu, H. Q.: Characterization of extracellular polymeric substances of aerobic and anaerobic sludge using three-dimensional excitation and emission matrix fluorescence spectroscopy, Water Res., 40 (6), 1233-1239, 2006.

Sheng, G. P., Yu, H. Q. and Li, X. Y.: Extracellular polymeric substances (EPS) of microbial aggregates in biological wastewater treatment systems: A review, Biotechnol. Adv., 28 (6), 882-894, 2010.

Stedmon, C. A., Markager, S. and Bro, R.: Tracing dissolved organic matter in aquatic environments using a new approach to fluorescence spectroscopy, Mar. Chem., 82, (3), 239-254, 2003.

Stedmon, C. A., Markager, S., Tranvik, L., Kronberg, L., Sl?tis, T. and Martinsen, W.: Photochemical production of ammonium and transformation of dissolved organic matter in the Baltic Sea, Mar. Chem., 104 (3-4), 227-240, 2007.

Tadini, A. M., Nicolodelli, G., Senesi, G. S., Ishida, D. A. and Milori, D. M. B. P.: Soil organic matter in podzol horizons of the Amazon region: Humification, recalcitrance, and dating, Sc. Total Environ., 613-614C, 160-167, 2017.

Vione, D., Falletti, G., Maurino, V., Minero, C., Pelizzetti, E., Malandrino, M., Ajassa, R., Olariu, R. I., Arsene, C.: Sources and sinks of hydroxyl radicals upon irradiation of natural water samples, Environ. Sci. Technol., 40 (12), 3775-3781, 2006.

Wan, D., Sharma, V. K., Liu, L., Zuo, Y. and Chen Y.: Mechanistic Insight into the Effect of Metal Ions on Photogeneration of Reactive Species from Dissolved Organic Matter, Environ. Sci. Technol., 53 (10), 5778-5786, 2019

Wang, K., Garg, S., and Waite, T. D.: Light-Mediated Reactive Oxygen Species Generation and Iron Redox Transformations in the Presence of Exudate from the Cyanobacterium Microcystis aeruginosa, Environ. Sci. Technol., 51, 8384 – 8395, 2017.

Ward, N. D., Keil, R. G., Medeiros, P. M., Brito, D. C., Cunha, A. C., Dittmar, T., Yager, P. L., Krusche, A. V. and Richey, J. E.: Degradation of terrestrially derived macromolecules in the Amazon River, Nat. Geosci., 6 (7), 530-533, 2013.

https://doi.org/10.5194/bg-2020-145
Preprint. Discussion started: 20 May 2020

Watanabe, S., Sudo, K., Nagashima, T., Takemura, T., Kawase, H. and Nozawa, T.: Future projections of surface UV-B in a changing climate. Geophys. Res.: Atmos. 2011, 116 (D16), 2011.

Wernberg, T., Bennett, S., Babcock, R. C., de Bettignies, T., Cure, K., Depczynski, M., Dufois, F., Fromont, J., Fulton, C. J., Hovey, R. K., Harvey, E. S., Holmes, T. H., Kendrick, G. A., Radford, B., Santana-Garcon, J., Saunders, B. J., Smale, D. A., Thomsen, M. S., Tuckett, C. A., Tuya, F., Vanderklift, M. A. and Wilson, S.: Climate-driven regime shift of a temperate marine ecosystem, Science, 353 (6295), 169-172, 2016.

Yamashita, Y. and Tanoue, E.: In situ production of chromophoric dissolved organic matter in coastal environments, Geophys. Res. Lett., 31 (14), L14302, 2004.

Yamashita, Y., Tanoue, E.: Chemical characterization of protein-like fluorophores in DOM in relation to aromatic amino acids, Mar. Chem., 82 (3-4), 255-271, 2003.

Yue, F. J., Li, S. L., Liu, C. Q., Mostofa, K. M. G., Yoshida, N., Toyoda, S., Wang, S. L., Hattori, S. and Liu, X. L.: Spatial variation of nitrogen cycling in a subtropical stratified impoundment in southwest China, elucidated by nitrous oxide isotopomer and nitrate isotopes. Inland Waters, 8 (7505), 1-10, 2018.

Zark, M. and Dittmar, T.: Universal molecular structures in natural dissolved organic matter, Nat. Commun., 9, (1), 3178. 2018.

Zhang, Y., Dijk, M. A., Van, Mingliang, L., Guangwei, Z. and Boqiang, Q.: The contribution of phytoplankton degradation to chromophoric dissolved organic matter (CDOM) in eutrophic shallow lakes: field and experimental evidence, Water Res., 43 (18), 4685-4697, 2009.

Zhu, Y. and Kieber, D. J.: Wavelength and temperature-dependent apparent quantum yields for photochemical production of carbonyl compounds in the North Pacific Ocean. Environ. Sci. Technol., 52, 1929-1939, 2018.

https://doi.org/10.5194/bg-2020-145
Preprint. Discussion started: 20 May 2020

Biogeosciences Discussions Open Access EGU

Table 1. Fluorescence EEM peaks wavelengths of the components identified in water samples collected from the Jingye lake on July 5 and October 12 at various sub-diurnal times.

Sampling time	Fluorescence peak (Ex/Em)											
	AHLS C-type		AHLS M-type		EPS				TLS or PLS		Newly-released PLS	
	Peak C	Peak A	Peak M	Peak A	Peak M	Peak A	Peak T	Peak Tuv	Peak T	Peak Tuv	Peak T	Peak Tuv
	(nm)											
Jingye lake (July 5, 2018)												
6:00 – 9:00					230/365	270/365	270/394	230/394				
10:00 – 15:00	315/418	260/418	305/383	220/383					270/338	225/338	285/357	240/357
16:00 – 20:00	325/430	260/430	300/379	240/379					265/338	220/338	280/351	
21:00 – 1:00	310/449	250/449							275/341	225/341		
2:00 – 6:00					270/364	230/364	270/400	230/400				
Jingye lake (Oct 12, 2018)												
6:00 – 9:00	310/418	260/418	305/394	220/394			285/352	235/352	265/336	220/336		
10:00 – 15:00	350/418	270/418	295/398	235/398			280/354	230/354	270/324	225/324		
16:00 – 20:00	335/430	265/430	295/382	235/382					270/336	225/336		
22:00 – 0:00	355/418	270/418	310/410	225/410	290/442	240/442	290/366	240/366	270/338	225/338		
2:00 – 6:00	355/430	270/430	315/428	225/428			280/374	230/374	270/336	225/336		

https://doi.org/10.5194/bg-2020-145
Preprint. Discussion started: 20 May 2020

722 Table 2. Fluorescence EEM peaks wavelengths of the components identified in water samples
723 collected from Jingye and Qingnian lakes in May and June at various sub-diurnal times.

Sampling time	Fluorescence peak (Ex/Em)											
	AHLS C-type		AHLS M-type		EPS				TLS or PLS		Newly-released PLS	
	Peak C	Peak A	Peak M	Peak A	Peak M	Peak A	Peak T	Peak Tuv	Peak T	Peak Tuv	Peak T	Peak Tuv
	(nm)											
Jingye lake (July 5, 2018)												
6:00 – 9:00					230/365	270/365	270/394	230/394				
10:00 – 15:00	315/418	260/418	305/383	220/383					270/338	225/338	285/357	240/357
16:00 – 20:00	325/430	260/430	300/379	240/379					265/338	220/338	280/351	
21:00 – 1:00	310/449	250/449							275/341	225/341		
2:00 – 6:00					270/364	230/364	270/400	230/400				
Jingye lake (Oct 12, 2018)												
6:00 – 9:00	310/418	260/418	305/394	220/394			285/352	235/352	265/336	220/336		
10:00 – 15:00	350/418	270/418	295/398	235/398			280/354	230/354	270/324	225/324		
16:00 – 20:00	335/430	265/430	295/382	235/382					270/336	225/336		
22:00 – 0:00	355/418	270/418	310/410	225/410	290/442	240/442	290/366	240/366	270/338	225/338		
2:00 – 6:00	355/430	270/430	315/428	225/428			280/374	230/374	270/336	225/336		

724

725
726
727
728
729
730
731
732
733
734
735
736
737
738
739
740
741
742
743
744
745
746
747
748
749
750
751
752
753

https://doi.org/10.5194/bg-2020-145
Preprint. Discussion started: 20 May 2020

754 Fig. 1. Fluorescence EEM images showing the peaks of fluorescent components identified in
755 diurnal water samples collected from Jingye lake on July 5, 2018. The EEM-PARAFAC model
756 was applied to each of the five sub-diurnal groups (6:00-9:00, 10:00-15:00, 16:00-20:00, 21:00-
757 1:00 and 2:00-6:00) of samples collected every hour, in order to illustrate the changes caused by
758 sunlight-induced and microbial degradation effects.

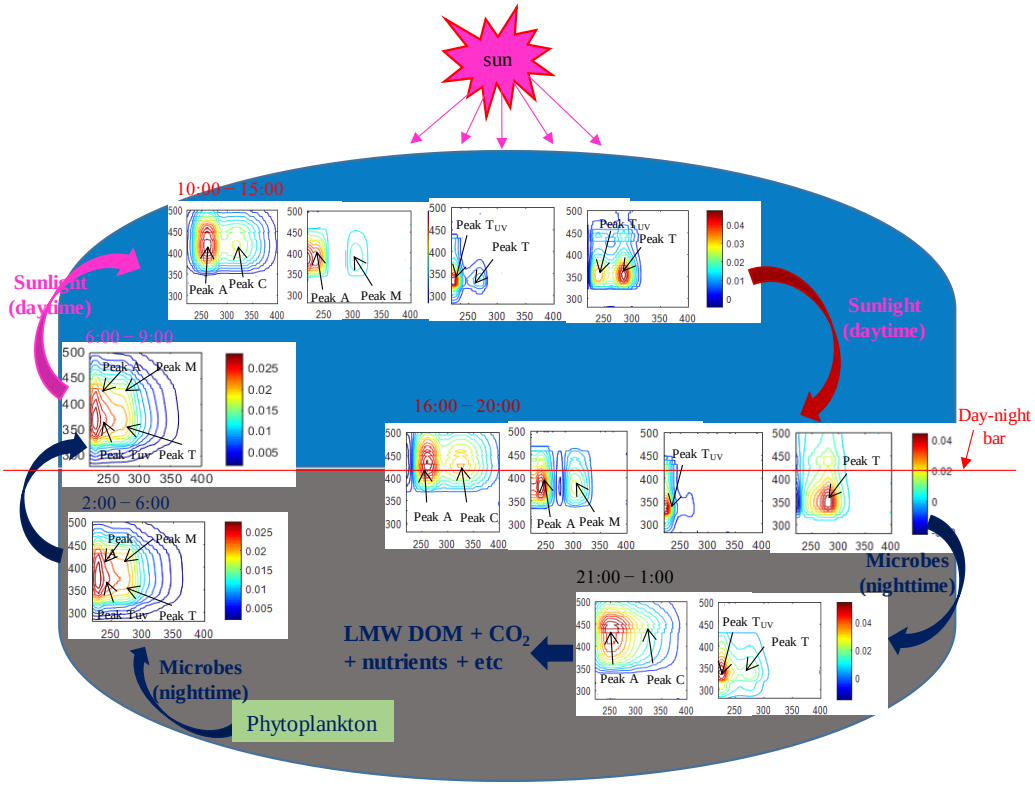

759
760
761
762
763
764

https://doi.org/10.5194/bg-2020-145
Preprint. Discussion started: 20 May 2020

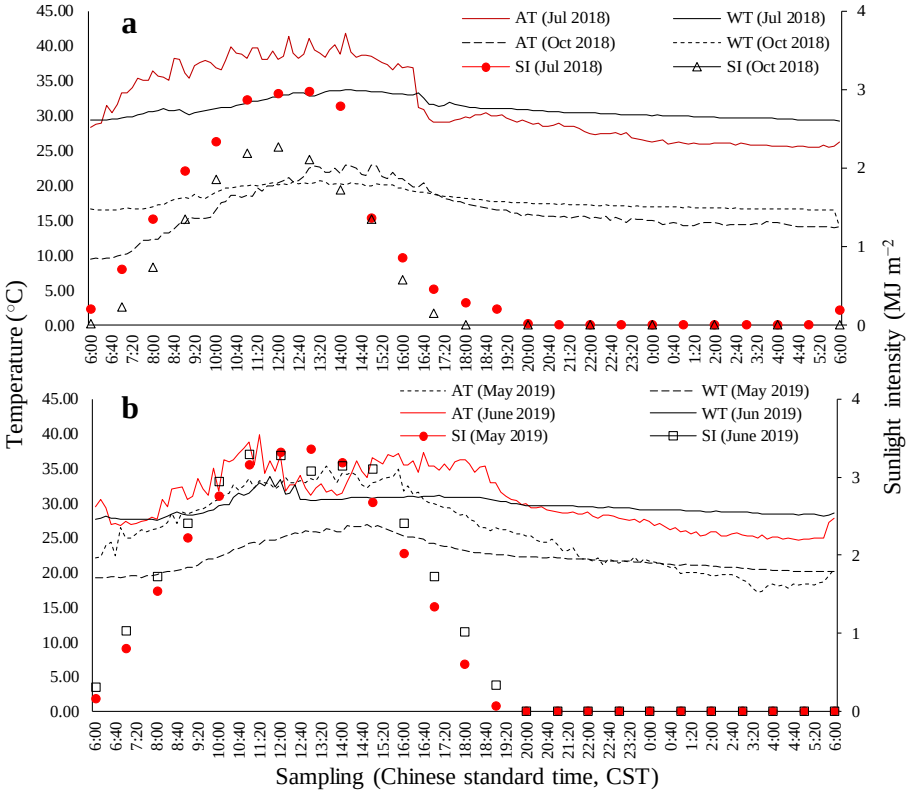

765 Fig. 2. Variation of air temperature (AT), water temperature (WT) and solar intensity in the
766 ambient environment of Jingye lake as a function of diurnal sampling time during July 5, 2018 (a),
767 and October 12, 2018 (b). Data were provided by Tianjin Meteorological Agency, Tianjin, China.

768

769

770

771

772

773

774

775

https://doi.org/10.5194/bg-2020-145
Preprint. Discussion started: 20 May 2020

Fig. 3. Fluorescence EEM images showing the peaks of fluorescent components identified in diurnal water samples collected from Jingye lake on Oct. 12, 2018. The EEM-PARAFAC model was applied individually to each of the five sub-diurnal groups (6:00-9:00, 10:00-15:00, 16:00-20:00, 21:00-1:00 and 2:00-6:00) of samples collected every hour, in order to illustrate the changes caused by sunlight-induced and microbial degradation effects.

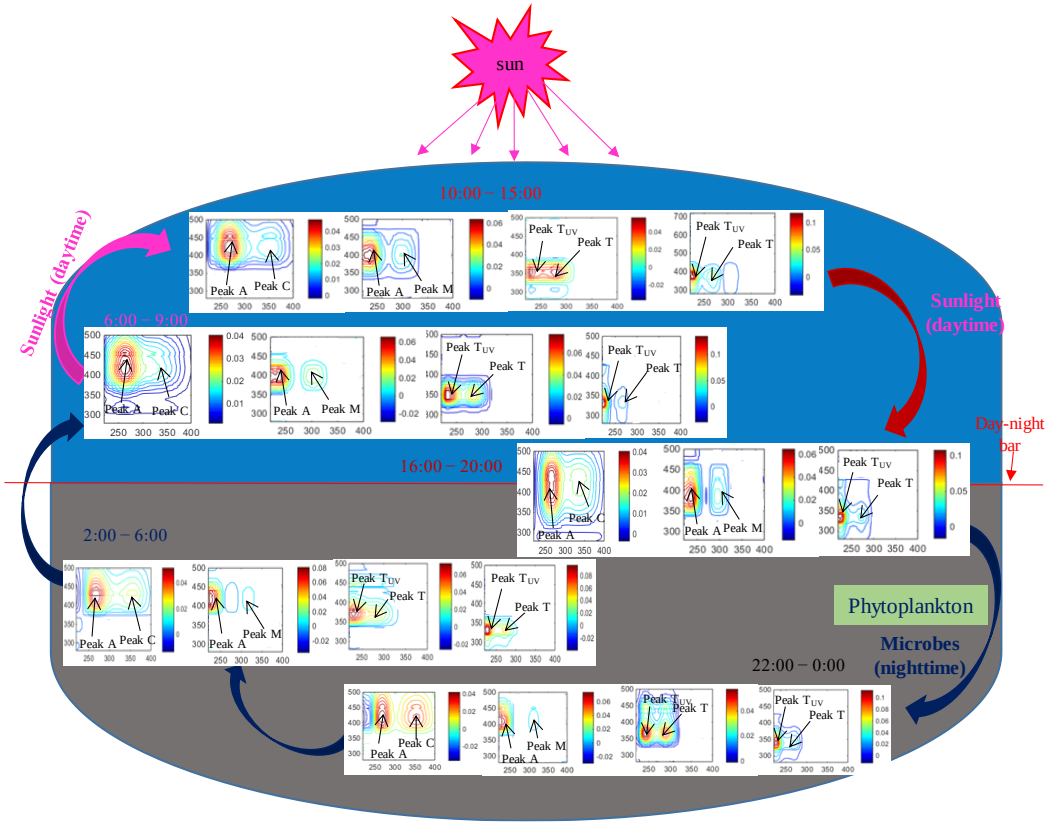

https://doi.org/10.5194/bg-2020-145
Preprint. Discussion started: 20 May 2020

788 Fig. 4. Fluorescence EEM images showing the peaks of fluorescent components identified in two
789 diurnal (6:00 and 14:00) water samples collected in triplicate from Jingye and Qingnian lakes on
790 May 2, 2019. The EEM-PARAFAC model was applied individually to each of the two sub-sample
791 groups collected at 6:00 and 14:00, in order to illustrate the changes depending on sunlight-induced
792 (14:00) and microbial (6:00) degradation effects.

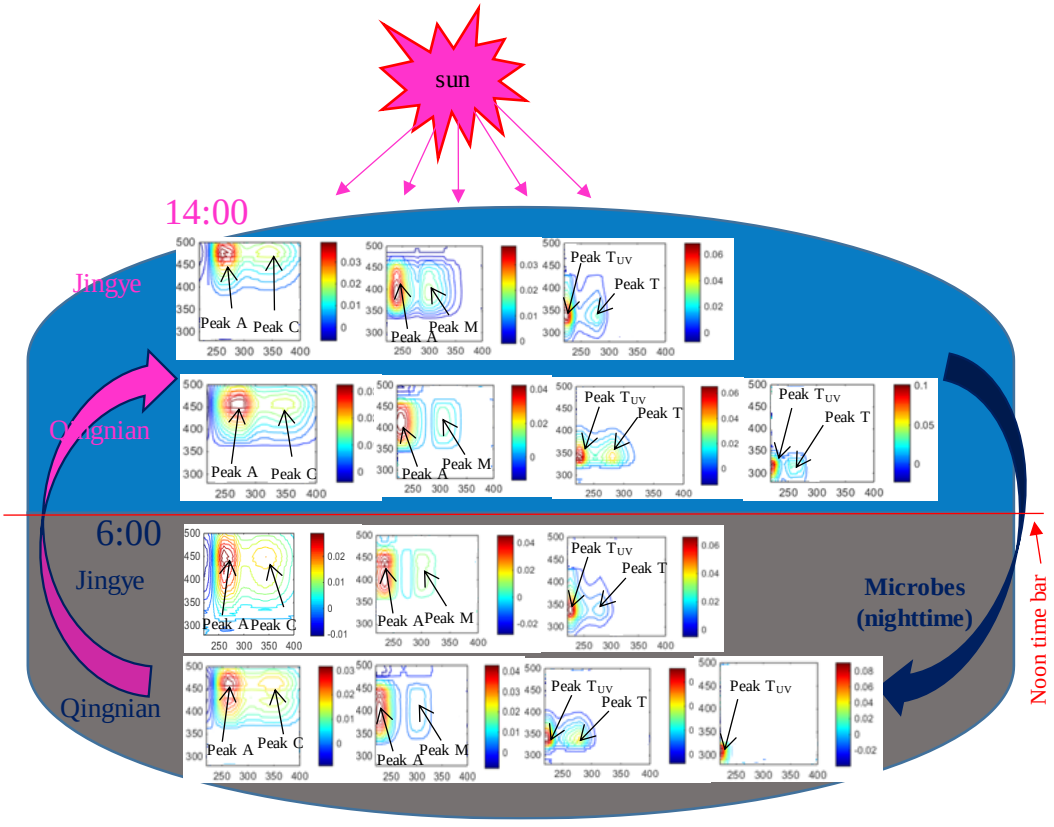

793
794
795
796
797
798
799

https://doi.org/10.5194/bg-2020-145
Preprint. Discussion started: 20 May 2020

Fig. 5. Fluorescence EEM images showing the peaks of fluorescent components identified in two diurnal (6:00 and 14:00) water samples collected in triplicate from Jingye and Qingnian lakes on June 30, 2019. The EEM-PARAFAC model was applied individually to each of the two sub-sample groups collected at 6:00 and 14:00, in order to illustrate the changes depending on sunlight-induced (14:00) and microbial (6:00) degradation effects.

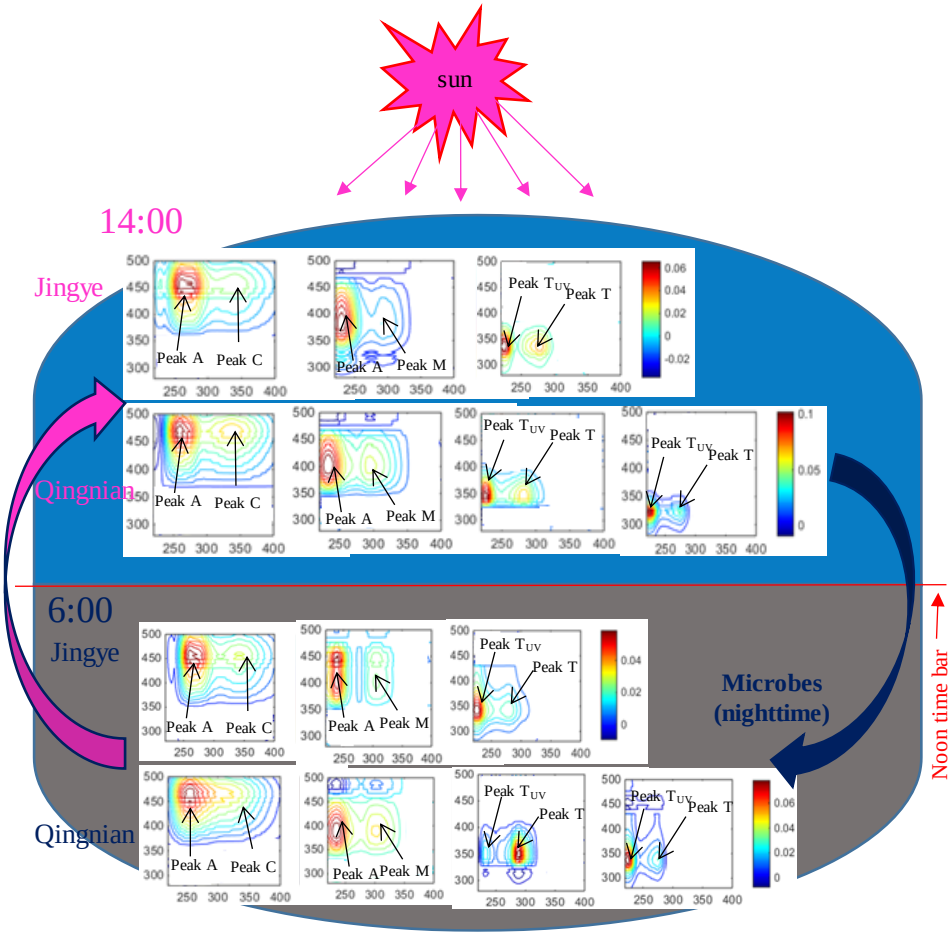

https://doi.org/10.5194/bg-2020-145
Preprint. Discussion started: 20 May 2020

Biogeosciences Discussions
Open Access
EGU

809 Fig. 6. Changes of nutrient concentrations in diurnal samples from Jingye lake: (a) nitrate (NO_3^-),
810 ammonium (NH_4^+), nitrite (NO_2^-) and dissolved organic nitrogen (DON), and (c) phosphates
811 (PO_4^{3-}) and dissolved silicon (DSi) collected in July; (b) NO_3^-, NH_4^+ and NO_2^- and (d) (PO_4^{3-}) and
812 DSi collected in October; and (e) dissolved organic carbon (DOC) collected in July and October.

https://doi.org/10.5194/bg-2020-145
Preprint. Discussion started: 20 May 2020

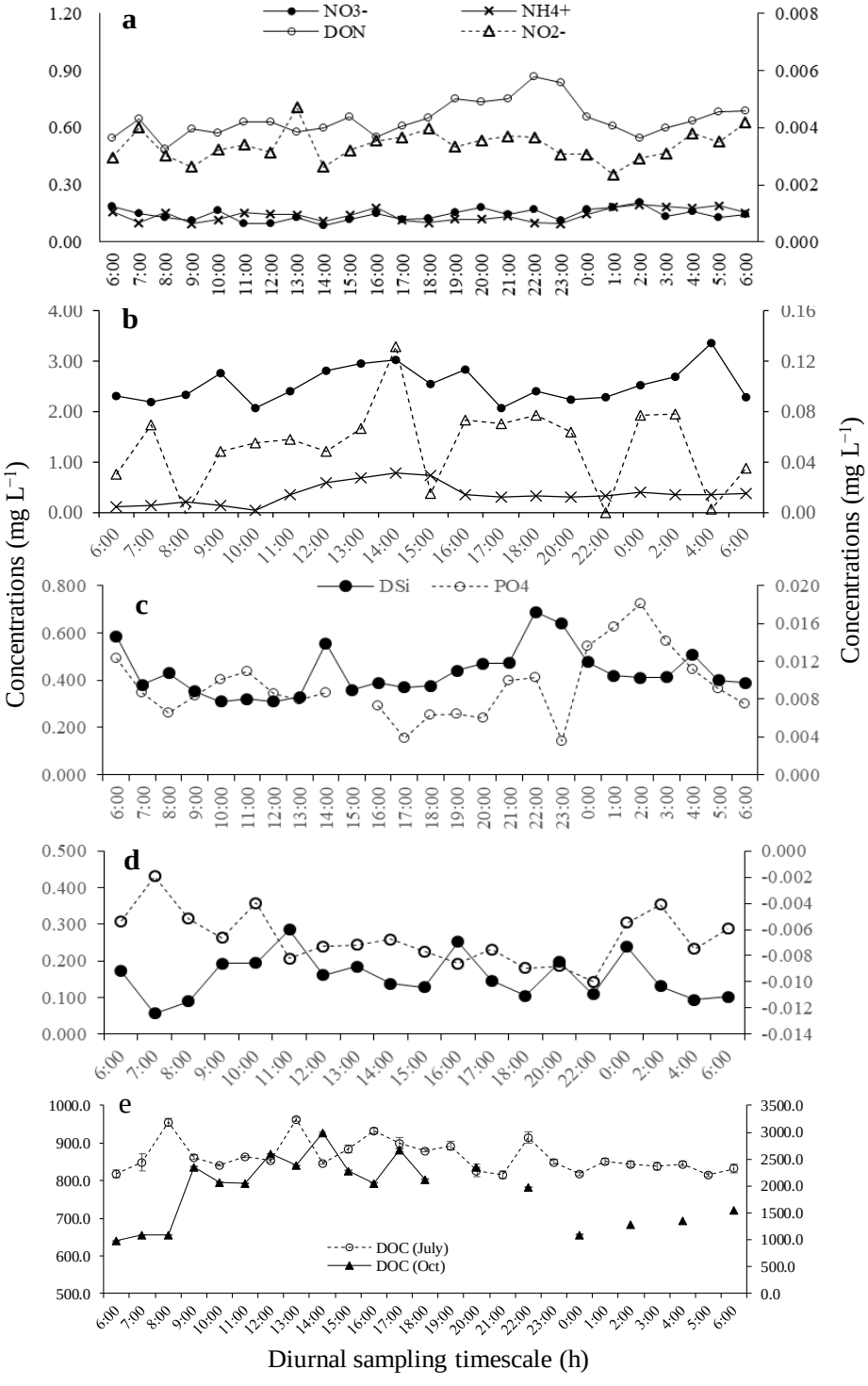

https://doi.org/10.5194/bg-2020-145
Preprint. Discussion started: 20 May 2020

Fig. 7. Flow diagram of the sequential production of autochthonous FDOM from phytoplankton and its subsequent degradation steps until complete mineralization under diurnal conditions as affected by sunlight-induced microbial-induced processes.

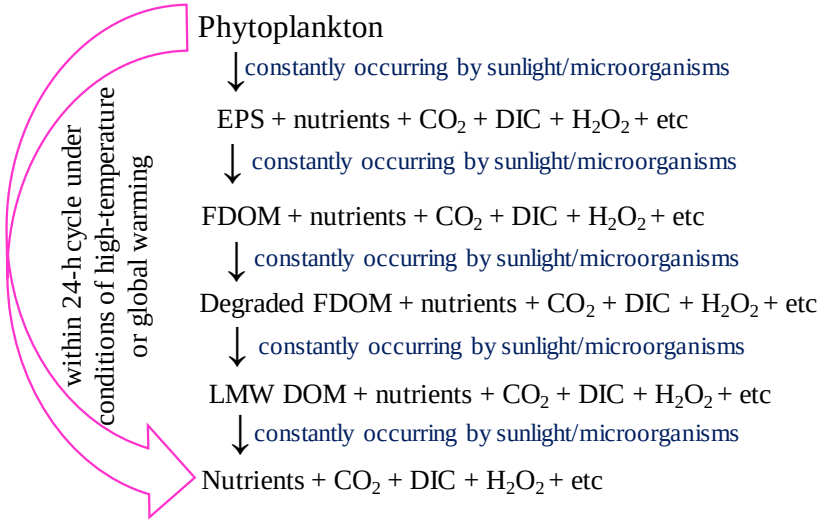

https://doi.org/10.5194/bg-2020-145
Preprint. Discussion started: 20 May 2020

829 Fig. 8. Pathways of generation and subsequent transformation of EPS into a combined form of C
830 and M types HLS that subsequently degrade into individual C-type AHLS and M-type AHLS,
831 which finally degrade to mineralization end-products.

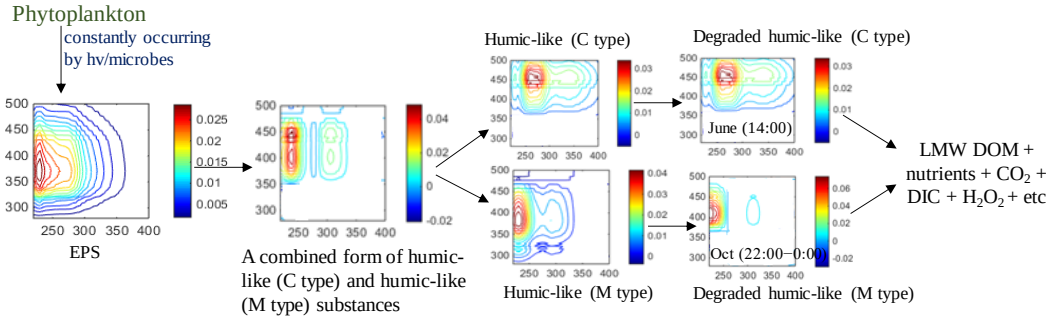

832
833
834
835
836
837
838
839
840
841
842
843
844
845
846
847

https://doi.org/10.5194/bg-2020-145
Preprint. Discussion started: 20 May 2020

Fig. 9. Pathways of generation and subsequent transformation of EPS into newly-released PLS that then convert into PLS which subsequently generate a combined form of TYLS, PALS and TLS that finally degrade to mineralization end-products.